Experimental evidence of Brillouin-induced polarization wheeling in highly birefringent optical fibers

Julien Fatome, Stéphane Pitois and Guy Millot

Institut Carnot de Bourgogne (ICB)
UMR 5209 CNRS-Université de Bourgogne, 9 av. Alain Savary, 21078 Dijon, France
jfatome@u-bourgogne.fr

Abstract: We study the influence of Stimulated Brillouin Scattering on the polarization stabilization of a light beam propagating in a highly-birefringent optical fiber. In particular, due to a saturation effect, we find that the output polarization lies on a ring when the polarization is represented onto the Poincaré sphere.

OCIS codes: (060.4370) Nonlinear optics, fibers; (230.4320) Nonlinear optical devices; (070.6020) Signal processing.

References and links

1. M. Martinelli, P. Martelli, and S. M. Pietralunga, "Polarization stabilization in optical communications systems," J. Lightwave Technol. **24**, 4172-4183 (2006).
2. B. Koch, A. Hidayat, H. Zhang, V. Mirvoda, M. Lichtinger, D. Sandel, and R. Noè, "Optical endless polarization stabilization at 9 krad/s with FPGA-based controller," IEEE Photon. Technol. Lett. **20**, 961-963 (2008).
3. S. Pitois, A. Sauter and G. Millot, "Simultaneous achievement of polarization attraction and Raman amplification in isotropic optical fibers", Opt. Lett. **29**, 599-601 (2004).
4. S. Pitois, J. Fatome, and G. Millot, "Polarization attraction using counter-propagating waves in optical fiber at telecommunication wavelengths," Opt. Express **16**, 6646-6651 (2008). http://www.opticsinfobase.org/oe/abstract.cfm?URI=oe-16-9-6646
5. L. Thevenaz, A. Zadok, A. Eyal and M. Tur, "All-optical polarization control through Brillouin amplification", in Optical Fiber Communication Conference, 2008 OSA Technical Digest CD (2008), paper OML7.
6. A. Zadok, E. Zilka, A. Eyal, L. Thévenaz, and M. Tur, "Vector analysis of stimulated Brillouin scattering amplification in standard single-mode fibers," Opt. Express **16**, 21692-21707 (2008). http://www.opticsinfobase.org/oe/abstract.cfm?URI=oe-16-26-21692
7. M. Martinelli, M. Cirigliano, M. Ferrario, L. Marazzi, and P. Martelli, "Evidence of Raman-induced polarization pulling," Opt. Express **17**, 947-955 (2009). http://www.opticsinfobase.org/oe/abstract.cfm?URI=oe-17-2-947
8. S. Wabnitz," Chiral polarization solitons in elliptically birefringent spun optical fibers", Opt. Lett. **34**, 908-910 (2009).
9. J.E. Heebner, R.S. Bennink, R.W. Boyd and R.A. Fisher, "Conversion of unpolarized light to polarized light with greater than 50% efficiency by photorefractive two-beam coupling", Opt. Lett. **25**, 257-259 (2000).
10. R.H. Chiao, B.P. Stoicheff and C.H. Townes, "Stimulated Brillouin scattering + coherent generation of intense hypersonic waves", Phys. Rev. Lett. **12**, 592-595 (1964).
11. G.P. Agrawal, *Nonlinear Fiber Optics, Third Edition*. 2001: San Fransisco, CA: Academic Press.
12. R.W. Hellwarth, "Theory of Stimulated Raman scattering", Phys. Rev. **130**, 1850-1852 (1963).

1. Introduction

In the optical communications and sensing communities, polarization is often an undesirable degree of liberty, which would need to be controlled as accurately as possible to guarantee high stability and reliability of the system [1]. There exist a large number of devices which allow light polarization control, and basically, we can make the distinction between dissipative and non-dissipative systems. Devices, such as Lefevre loops, half-wave or quarter-

#111406 - $15.00 USD Received 14 May 2009; revised 6 Jul 2009; accepted 7 Jul 2009; published 10 Jul 2009

wave plates, which usually allow us to transform any input state of polarization into another without any loss, define the non-dissipative elements. Unfortunately, the output polarization directly depends on the input and thus, the polarization fluctuations at the output of the system are the same as the input. To maintain a constant and fixed output polarization state, standard polarizers, such as Glan polarizers, can be used. These devices are qualified as dissipative elements in the sense that the intrinsic losses depend on the input polarization. Although the output polarization state is fixed by the device, the main drawback is that input polarization fluctuations are now transformed into intensity fluctuations. In order to achieve both constant output polarization and intensity, opto-electronic devices based on an active-feedback polarization control have been developed [1-2]. Nevertheless, these systems usually involve complex set-up and are often not fast enough to respond efficiently to ultrashort polarization variations.

To overcome this practical issue, all-optical polarization control by means of nonlinear effects is an interesting physical approach of both fundamental and applicative interests. Some recent works have demonstrated theoretically and experimentally the possibility of manipulating light polarization thanks to nonlinear effects occurring in optical fibers [3-8] or photorefractive crystals [9]. For example, in Refs. [3-4], Pitois *et al.* have demonstrated that a polarization attraction effect can be obtained by launching two intense counter-propagating waves in an isotropic optical fiber. More recently, Thevenaz *et al.* [5-6] and Martinelli *et al.* [7] have reported polarization pulling effects induced either by Brillouin or stimulated Raman scattering in randomly birefringent fibers. In this work, we consider a light beam propagating in a nonlinear highly-birefringent (Hi-Bi) optical fiber with arbitrary initial polarization. We show both theoretically and experimentally that Brillouin effect, by means of a saturation process and combined with a polarizer, can induce a stabilization of the polarization emerging from the Hi-Bi fiber. In particular, we demonstrate that output polarization lies on a ring when polarization is represented on the Poincaré sphere.

2. Theoretical considerations

It is well known that when an optical fiber is pumped by a continuous or a quasi-continuous wave having a spectral width smaller than the typical Brillouin bandwidth $\Delta\nu_B$, most of the incident energy is back-scattered. Consequently, due to the generation of a backward-propagating Stokes wave, only a small part of the initial intensity emerges from the fiber [10-11]. An important property of this stimulated Brillouin scattering (SBS) effect in silica optical fibers is that it usually occurs at very low input power levels, compared for example to the power levels needed for stimulated Raman scattering [11-12]. In this work, we take advantage of this property to observe a stabilization of light polarization emerging from a high-birefringence optical fiber thanks to a SBS-induced saturation process.

Let us begin by demonstrating that the physical process under study can be easily understood using a simple model for the Brillouin saturation effect. The system under consideration is a standard high-birefringence fiber having two principal axes denoted *x* (slow axis) and *y* (fast axis). First, we assume that, regarding the Brillouin effect, the two fiber axes can be considered as two independent systems (i.e. light polarized along the slow (fast) axis of the fiber generates SBS only along this axis). We also make the assumption that the generation of higher-order Brillouin Stokes bands can be neglected. This hypothesis is indeed confirmed by the experimental observations. In this context, we now consider that the optical power at the output of the fiber can be simply modeled using the following relations:

$$P_x^{out} = P_{sat} \times \tanh(\alpha\, P_x^{in} / P_{sat}), \quad (1)$$

$$P_y^{out} = P_{sat} \times \tanh(\alpha\, P_y^{in} / P_{sat}), \quad (2)$$

where P_x^{out} and P_y^{out} are the output powers along the *x*- and *y*-axis of the fiber, respectively and P_{sat} the output saturation power due to Brillouin back-scattering. α is a coefficient taking account for fiber losses. Note that the analytical expression of Eqs. (1) and (2) was empirically

#111406 - $15.00 USD Received 14 May 2009; revised 6 Jul 2009; accepted 7 Jul 2009; published 10 Jul 2009

determined by means of our experimental measurements presented in Fig. 1. More precisely, figure 1a represents the experimental transmitted power as well as the back-scattered power as a function of the input average power injected into the 500-m long Hi-Bi fiber used in our experiment. The blue (black) lines show the results obtained by injecting light along the slow (fast) axis of the Hi-Bi fiber. As can be seen, the saturation occurs for input powers larger than 75 mW while the transmitted power saturates around 8 mW. Figure 1b shows that the theoretical transmitted power (blue line) obtained from the simple model provided by equations (1) and (2) fit very well the experimental behavior. Note that the saturation power P_{sat} and losses coefficient α were both adjusted to match the experimental values.

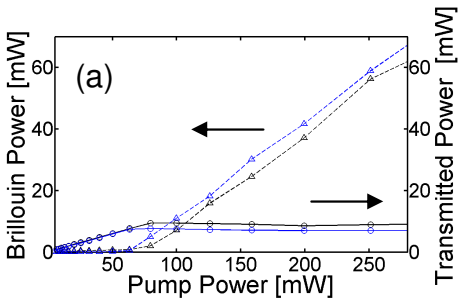

Fig. 1. (a) Experimental transmitted (triangles) and back-scattered Brillouin (circles) powers as a function of the input power for the fast (blue lines) and slow (black lines) axes of the 500-m long Hi-Bi fiber.

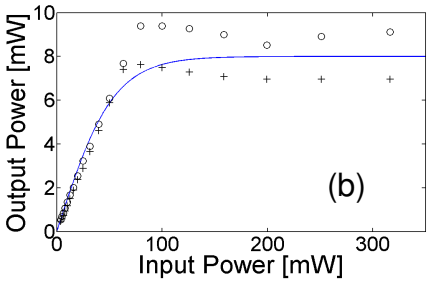

Fig. 1. (b) Theoretical transmitted power (blue line) as a function of the input power compared to the experimental data (circles and crosses).

Then, it is interesting to consider the consequence of the Brillouin-induced power saturation in terms of output polarization. To this aim, it may be convenient to represent light polarization onto the Poincaré sphere thanks to the usual three-component Stokes vectors defined as:

$$\begin{cases} S_1 = P_x - P_y \\ S_2 = 2\sqrt{P_x P_y}\cos(\varphi) \\ S_3 = 2\sqrt{P_x P_y}\sin(\varphi) \end{cases} \tag{3}$$

where φ is the phase difference between the two axes. Combining relations (1) with equations (3) leads to the following set of Stokes components:

$$\begin{cases} S_1 = P_{sat}\left[\tanh(\alpha P_x^{in}/P_{sat}) - \tanh(\alpha P_y^{in}/P_{sat})\right] \\ S_2 = 2P_{sat}\sqrt{\tanh(\alpha P_x^{in}/P_{sat})\times\tanh(\alpha P_y^{in}/P_{sat})}\cos(\varphi) \\ S_3 = 2P_{sat}\sqrt{\tanh(\alpha P_x^{in}/P_{sat})\times\tanh(\alpha P_y^{in}/P_{sat})}\sin(\varphi). \end{cases} \tag{4}$$

An interesting situation occurs when both $P_x^{in} >> P_{sat}$ and $P_y^{in} >> P_{sat}$. In this case, it is indeed straightforward to show that the output light polarization can be written as:

$$\begin{cases} S_1 \to 0 \\ S_2 \to 2P_{sat}\cos(\varphi) \\ S_3 \to 2P_{sat}\sin(\varphi) \end{cases} \tag{5}$$

where φ could take an infinity of different values between 0 and 2π (which is typically the case when the signal polarization is scrambled). Consequently, for large input powers, one can

#111406 - $15.00 USD Received 14 May 2009; revised 6 Jul 2009; accepted 7 Jul 2009; published 10 Jul 2009

easily see that the output polarization will lie on a ring ("a wheel") on the Poincaré sphere. This ring is indeed associated with polarization states which satisfy $P_x^{out}=P_y^{out}=P_{sat}$, a condition favored by the Brillouin induced power saturation effect occurring on both axes of the Hi-Bi fiber. As a result, for large input powers, and whatever the initial signal polarization state, if a polarizer is aligned along one of the output axes of the fiber, both intensity and polarization states should be stabilized. This Brillouin-induced polarization wheeling is illustrated in Figs. 2a and 2b which show the input and output polarizations calculated numerically for an initial scrambled signal when the input power is large enough, compared to the Brillouin threshold. As can be seen in Fig. 2b, due to the Brillouin-induced saturation, whatever the initial power distribution, the optical power tends to be equal on both axes (S_1 = 0). On the other hand, the phase difference between the two axes taking a large number of different values due to the initial scrambling, almost all output states are localized around a ring onto the Poincaré sphere.

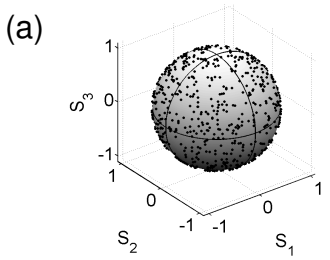

Fig. 2(a). Polarization of the input scrambled signal plotted on the Poincaré sphere.

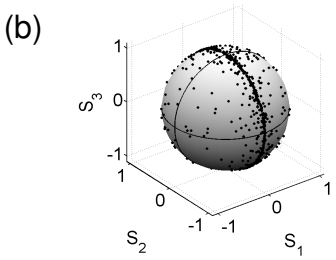

Fig. 2(b). Polarization of the output signal plotted on the Poincaré sphere.

3. Experimental set-up

The experimental set-up employed to observe the Brillouin-induced polarization wheeling is represented in Fig. 3. The signal source is delivered by means of a tunable external-cavity laser emitting around 1555 nm. A polarization scrambler is used to periodically and randomly change the polarization state of the light (repetition rate of 5 kHz). The resulting signal is then amplified thanks to a 30-dBm Erbium-doped fiber amplifier (EDFA) before injection into a Hi-Bi fiber. The first fiber under-test was a 500-m long polarization maintaining highly nonlinear fiber (PM-HNLF) previously characterized in Fig. 1. The parameters are an effective area of 13 μm^2, an attenuation of 0.77 dB/km, chromatic dispersion of -1.3 ps/nm/km at 1550 nm, a beat length of 4.3 mm and a measured Brillouin threshold of 75 mW, (see Fig. 1). The second fiber under-test was a 200 m-long polarization maintaining highly non-linear photonic crystal fiber (PM-PCF) provided by PERFOS. The parameters are an effective area of 3 μm^2, an attenuation of 14.3 dB/km, chromatic dispersion of 110 ps/nm/km at 1550 nm, a beat length of 1.3 mm and a measured Brillouin threshold of 200 mW.

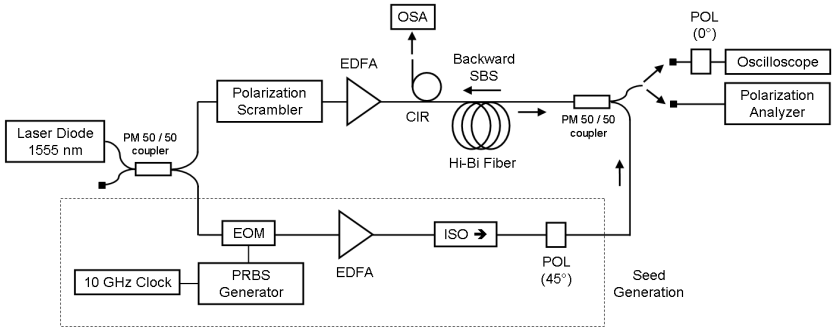

Fig. 3. Experimental set-up. CIR: Circulator, EDFA: Erbium-doped Fiber Amplifier, EOM: Electro-optic modulator, POL: Polarizer, ISO: Optical isolator, PRBS: Pseudo-random bit sequence, OSA: Optical Spectrum Analyzer.

#111406 - $15.00 USD Received 14 May 2009; revised 6 Jul 2009; accepted 7 Jul 2009; published 10 Jul 2009

A circulator was also inserted between the EDFA and the fiber input in order to monitor the back-scattered light. At the output of the fiber, the emerging light was analyzed thanks to a commercially available polarization analyzer. The temporal intensity profile after a polarizer aligned along the slow axis of the fiber under-test was also recorded by means of a photodiode and an oscilloscope. Figures 4a and 4b show the experimental output polarizations represented on the Poincaré sphere at low and high powers when the signal is injected into the PM-HNLF. Far below the Brillouin threshold (10 mW, Fig. 4a), the propagation is linear and the Poincaré sphere is entire covered due to the scrambling process. At the opposite, when the input power is increased far above the Brillouin threshold (400 mW, Fig. 4b), the formation of a ring is clearly visible in good concordance with numerical predictions of Fig. 2. As shown in Figs. 5a and 5b, similar results were obtained in the 200-m long PM-PCF for an input average power of 1.1 W. We would like to emphasize that the few dots outside the ring correspond to initial polarizations which are nearly aligned with one of the fiber principal axis. In that case, optical power on the orthogonal axis is indeed too low to obtain the saturation effect. Even if the initial power asymmetry is reduced after propagation, a significant power difference between the two axes can still be observed at the output of the fiber.

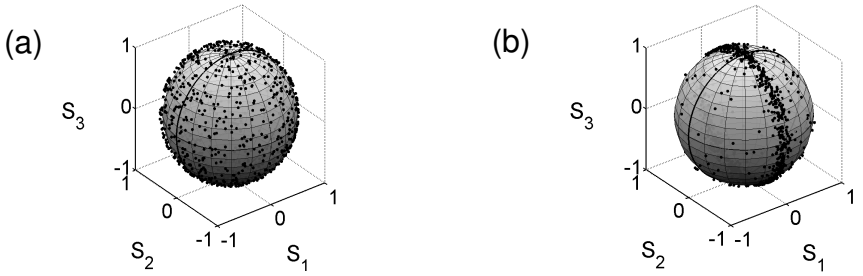

Fig. 4. Output polarization of the scrambled signal after propagation in the 500-m long PM-HNLF for an input average power of (a) 10 mW and (b) 400 mW.

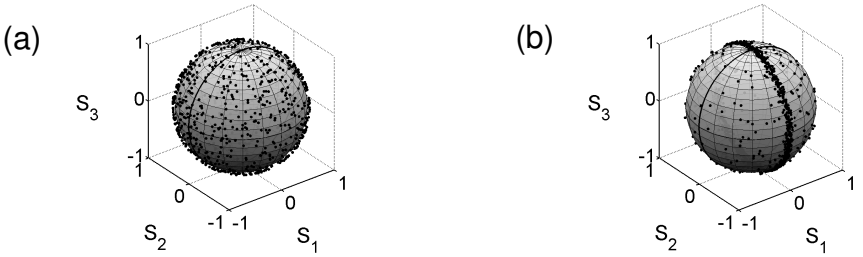

Fig. 5. Output polarization of the scrambled signal after propagation in the 200-m long PM-PCF for an input average power of (a) 100 mW and (b) 1100 mW.

Figures 6a, b and c illustrate the polarization of the back-scattered laser beam. At low power, far below the Brillouin threshold (10 mW Fig. 6a), the harvested light is essentially a reflection on the input connector and thus is equivalent to the input scrambled signal. When the power is increased above the Brillouin threshold, we can observe the formation of a polarization cigar having a degree of polarization close to zero at the center of the Poincaré sphere and close to one at both cigar ends. This cigar shape could be explained by the fact that, at z = 0, the back-scattered light due to SBS can be modeled as a superposition of orthogonaly-polarized photons generated at different positions of the fiber. As the coherence length of the ECL used in the experiment was only in the order of a few meters, light at z = 0 can be represented by the sum of a large number of mutually incoherent orthogonaly-polarized contributions. On the Poincaré sphere, and for a great number of contributions, the resulting polarization lies on a line passing by $S_1 = +1$ and $S_1 = -1$, these two particular dots representing the principal axes of the fiber. Note that the point at the center of the cigar (or center of the sphere), where the DOP is exactly equal to zero, corresponds to the superposition

#111406 - $15.00 USD Received 14 May 2009; revised 6 Jul 2009; accepted 7 Jul 2009; published 10 Jul 2009

of waves mutually incoherent and having identical average powers along the two axes of the fiber.

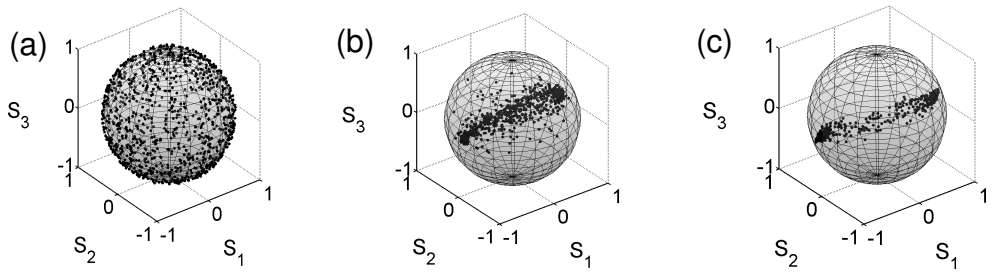

Fig. 6. Polarization of the back-scattered signal generated into the 500-m long PM-HNLF for an input average power of (a) 10 mW and (b) 150 mW (c) Same as (b) but for the 200-m long PCF and an input average power of 250 mW.

Finally, we have studied the ability of the Brillouin induced polarization wheeling to stabilize the output polarization and intensity by inserting a polarizer at the PM-HNLF output, aligned along the slow axis. Temporal intensity profiles monitored at the output of the polarizer are represented in Fig. 7a. At low power (10 mW, blue line), large fluctuations of the intensity are observed due to the initial polarization scrambling. Note that light polarization is changed at a repetition rate of 5 kHz. As the initial power is increased up to 400 mW, the wheeling polarization effect occurs so that a significant reduction of the polarization fluctuations is observed (black line). Nevertheless, one can now observe that fast noisy intensity fluctuations appear on the intensity profile. In fact, these fluctuations are inherent to the random nature of spontaneous Brillouin scattering (SBS). At this point, it may be important to precise that the fluctuations observed on the two curves in Fig. 7a do not have the same origin. The fluctuations of the blue curve (small power) are associated with polarization fluctuations (introduced by the polarization scrambling) whereas the fluctuations observed at high power (black line) only originate from SBS-induced intensity noise and the reduction of the polarization fluctuations have to be observed by looking at the mean value of the curve. To limit this phenomenon, we have seeded the SBS effect, so that to stabilize the scattering process. In this aim, a few milliwatt seed-signal, which frequency corresponds to the first Brillouin Stokes, was injected into the fiber under-test thanks to a counter-propagating configuration (see the experimental set-up in Fig. 3). The seed-signal was obtained from the same laser diode and modulated in intensity by means of a pseudo-random bit sequence generator and an electro-optic modulator so as to generate a sideband corresponding to the first Brillouin Stokes wavelength generated in the Hi-Bi fiber. The clock frequency (9.706 GHz for the PM-HNLF and 10.451 GHz for the PM-PCF) was carefully adjusted so as to maximize the Brillouin amplification of the counter-propagating seed-signal. Output intensity profile in presence of the seed-signal was plotted in Fig. 7b (red line) and shows a significant reduction of the fast fluctuations.

#111406 - $15.00 USD Received 14 May 2009; revised 6 Jul 2009; accepted 7 Jul 2009; published 10 Jul 2009

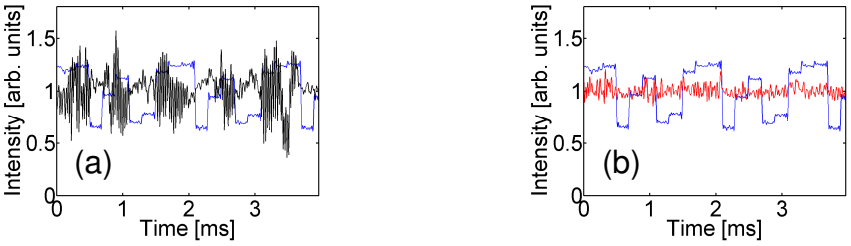

Fig. 7. (a) Output intensity profile of the scrambled signal propagating into the 500-m long PM-HNLF and passing through a polarizer, for an input average power of 10 mW (blue line) and 400 mW (black line) (b) same as (a) but in presence of a counter-propagating seed-signal.

Finally, Figs. 8 show the temporal intensity profiles recorded at the output of the 200-m long PM-PCF, after the polarizer, and in presence of a counter-propagating seed-signal. The resulting signals are monitored by means of the "persistence" mode of the oscilloscope for an input average power of 10 mW (a) and 400 mW (b). At low power, large fluctuations due to the polarization scrambling are clearly observed and, as expected, these fluctuations are uniformly distributed. On the other hand, for an input average power of 400 mW, thanks to the Brillouin-induced polarization wheeling, a significant reduction of these intensity fluctuations is clearly observed, demonstrating the ability of this technique to stabilize both polarization and intensity.

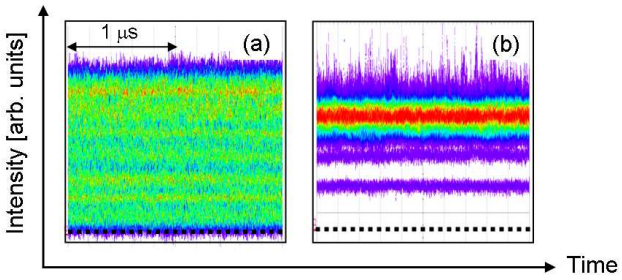

Fig. 8. (a) Intensity profile of the scrambled signal propagating into the 200-m long PM-PCF in presence of a counter-propagating seed-signal and recorded after the polarizer (a) for an input average power of 10 mW (b) 400 mW.

4. Conclusion

In conclusion, we have observed that a Brillouin-induced saturation process can lead to a stabilization of light polarization in highly-birefringent optical fibers. This effect is characterized by the formation of a "wheel" on the Poincaré sphere, corresponding to an equalization of the optical powers propagating along the two fiber axes. Combined with an output polarizer, this system allows an all-optical control and stabilization of light polarization which we believe could find many applications in the optical communication or sensor field.

Acknowledgment

We would like to thank PERFOS (www.perfos.com) for providing the PCF and the Agence National de la Recherche (ANR), 2006 TCOM 016 FUTUR project, for financial support.

#111406 - $15.00 USD Received 14 May 2009; revised 6 Jul 2009; accepted 7 Jul 2009; published 10 Jul 2009